Simulation of Semiconductor Processes and Devices 2016
Edited by E. Bär, J. Lorenz, and P. Pichler

Modeling the Thermal Conductivity of Si Nanowires with Surface Roughness

Kantawong Vuttivorakulchai, Mathieu Luisier, and Andreas Schenk
Integrated Systems Laboratory, ETH Zurich, CH-8092 Zurich, Switzerland.
E-mail: kvuttivo@iis.ee.ethz.ch

***Abstract*—Good thermoelectric devices with a high value of figure of merit are required to convert back waste heat into useful energy. One way to achieve this goal is to engineer the surface of nanostructures by introducing roughness, thus leading to a significant reduction of their thermal conductivity. We formulate here new theoretical descriptions of phonon interface roughness scattering in Si nanowires with a surface distributed either according to a Gaussian or exponential correlation function. Our calculations of the thermal conductivity of Si nanowires show an excellent agreement with experimental data. It is further demonstrated that the distribution of the nanowire surface (Gaussian or exponential) has almost no influence on the thermal conductivity. We finally predict that the thermal conductivity depends on the nanowire crystal orientation with a lower value along the ⟨100⟩ rather than the ⟨111⟩ direction. The developed scheme can now be used to model the thermal conductivity of other materials as well.**

Keywords—thermoelectricity; thermal conductivity; phonon surface roughness; device modeling

I. INTRODUCTION

About two-third of the global energy production is lost as waste heat. Thermoelectric materials with a high figure of merit (ZT) are therefore long-desired to directly and reversibly convert heat back into useable electrical energy. So far the highest ZT value has been found in bulk SnSe due to its intrinsically ultra-low lattice thermal conductivity [1]. More common materials could also exhibit a high ZT value if they were patterned as nanostructures and their surface properly engineered. For instance, nanowires with a rough surface exhibit ZT 100× higher than in bulk due to their reduced lattice thermal conductivity [2,3]. In this work we model such devices by introducing a new way of calculating the thermal conductivity of nanowires with surface roughness. The model is applied to nanowires with diameters below 150 nm and different directions of heat propagation. Good agreements with experimental data validate our approach.

II. THEORY AND APPROACH

We use the valence-force-field (VFF) method and the parameterization from Ref. [4] to calculate bulk phonon band structures. The latter are used as inputs to evaluate the thermal conductivity of nanowires through the Landauer formula for diffusive heat transport [5]. The phonon lifetimes corresponding to each relevant scattering process, e.g. anharmonicity, impurity, and boundary scattering are obtained by fitting the bulk properties of Si. As a next step, these fitting parameters are used to predict the thermal conductivity of nanowires. No further adjustable parameter is required.

To properly account for interface roughness scattering, we follow the derivation of the rate of scattering by a static strain field [6] and use Fermi's Golden Rule to determine the transition probability per unit time. A matrix element for the perturbed Hamiltonian due to space dilatation can be derived from that. In our calculations, transitions are allowed between all acoustic and optical phonon branches. An additional Bose-Einstein thermal variation of the surface roughness scattering rate has been removed from the expression in Ref. [7] according to the derivation given in Ref. [6]. Two new expressions for the Fourier transformation of the dilatation are derived for the case of a rough surface given by an exponential- and a Gaussian-autocorrelation function. These expressions depend on the root mean square height (Δ) of the roughness fluctuations and on its correlation length (L). A previous study showed that experimental data can be slightly better fitted with an exponential autocorrelation function [8].

A. Phonon band structure of Si

We use the VFF model based on an extension of Keating's approach [4]. The lattice potential energy is expressed in terms of atomic locations. It is found that only four types of these interactions are necessary to well reproduce the Si phonon dispersion. The short-range interaction potential includes the following four terms

$$\begin{aligned} U = & \sum_i \sum_{j\in NN(i)} \frac{\alpha_{ij}}{b_{ij}^2}\left(\boldsymbol{r}_{ij}^2 - \boldsymbol{b}_{ij}^2\right)^2 \\ & + \sum_i \sum_{j\in NN(i)} \sum_{k\in NN(i)}^{k\neq j} \frac{\beta_{jik}}{b_{ij}b_{ik}}\left(\boldsymbol{r}_{ij}\cdot\boldsymbol{r}_{ik} - \boldsymbol{b}_{ij}\cdot\boldsymbol{b}_{ik}\right)^2 \\ & + \sum_i \sum_{j\in NN(i)} \sum_{k\in NN(i)}^{k\neq j} \frac{\chi_{jik}}{b_{ij}b_{ik}}\left(\boldsymbol{r}_{ij}^2 - \boldsymbol{b}_{ij}^2\right)\left(\boldsymbol{r}_{ik}^2 - \boldsymbol{b}_{ik}^2\right) \\ & + \sum_i \sum_{j\in NN(i)} \sum_{k\in NN(i)}^{k\neq j} \sum_{l\in NN(k)}^{COP,l\neq i} \frac{\kappa_{jikl}}{\sqrt{b_{ij}b_{ik}b_{ki}b_{kl}}} \\ & \left(\boldsymbol{r}_{ij}\cdot\boldsymbol{r}_{ik} - \boldsymbol{b}_{ij}\cdot\boldsymbol{b}_{ik}\right)\left(\boldsymbol{r}_{ki}\cdot\boldsymbol{r}_{kl} - \boldsymbol{b}_{ki}\cdot\boldsymbol{b}_{kl}\right) \end{aligned} \quad (1)$$

where $\boldsymbol{r}_{ji} = \boldsymbol{r}_j - \boldsymbol{r}_i$ is the bond vector connecting atoms i and j. In the absence of long-range potentials such as Coulomb

978-1-5090-0818-6/16/$31.00 ©2016 IEEE

interaction, b_{ij} is equal to the equilibrium bond length. The variable COP denotes the coplanar plane of the bonds linkage among atoms j, i, k, and l. The potential parameters (α, β, χ, and κ) are short-range force constants corresponding to bond stretching, bond bending, cross-stretch interactions, and coplanar bend-bend interactions, respectively.

The phonon equation of motion can be written as

$$\sum_{\sigma,\eta'} D_{\rho,\sigma}(\eta\eta'|\boldsymbol{q})\, w_{n\sigma}(\eta'|\boldsymbol{q}) = \omega_n^2(\boldsymbol{q})\, w_{n\rho}(\eta|\boldsymbol{q}). \quad (2)$$

Here η is an atom index inside a unit cell, while ρ and σ refer to the Cartesian coordinates. The phonon frequencies and eigenvectors are ω_n and $w_{n\rho}$, respectively, for phonon branch n and wave vector $\boldsymbol{q}$. Finally, D is the dynamical matrix of the system with its non-zero entries defined as

$$D_{\rho,\sigma}(\eta\eta'|\boldsymbol{q}) = \frac{1}{\sqrt{M_\eta M_{\eta'}}} \sum_{l'} \Phi_{\rho,\sigma}(l\eta|l'\eta')\, \mathrm{e}^{-i\boldsymbol{q}\cdot[r(l\eta)-r(l'\eta')]} . \quad (3)$$

In Eq. (3) M is the atom mass and l the unit cell index of the simulated structure. The atom force constant matrix (Φ) contains the following elements:

$$\Phi_{\rho,\sigma}(i|j) = \left.\frac{\partial^2 U}{\partial r_{i\rho}\partial r_{j\sigma}}\right|_b . \quad (4)$$

The value of the potential parameters α, β, χ, and κ is adjusted till the phonon frequencies resulting from the eigenvalue problem in Eq. (2) fit experimental data in the best possible way, as shown in Fig. 1.

B. Thermal conductivity

The computational burden to obtain the full-band phonon dispersion and thermal conductivity of the studied Si nanowires is much too large to be of practical usage. We therefore have to rely on bulk-like properties to estimate the nanowire ones. Going the other way around, i.e. extrapolating the thermal conductivity of large nanowires from very small ones has also been proposed [5]. In our approach we extract a bulk unit cell from nanowires and change the orientation of this unit cell according to the nanowire growth direction. The phonon dispersion can then be computed. The transport direction is aligned with the x-axis in all cases. The wave vector $\boldsymbol{q}$ in the first Brillouin Zone (BZ) is discretized with 201 points along the x-axis and 51 in the others. Note that a square unit cell is created resulting in a BZ with the same shape. The diffusive Landauer formula for thermal conductivity is used as follows

$$k_{ph} = \frac{1}{A}\int M(\omega)\lambda(\omega)\frac{\hbar\omega}{2\pi}\frac{\partial n_0}{\partial T}d\omega . \quad (5)$$

From the bandstructure we extract the number of states crossing a given energy (frequency) along the x-axis to obtain $M(\omega)$, the frequency-dependent ballistic transmission probability. In Eq. (5) T is the lattice temperature, A the cross-sectional area of the conductor, and n_0 the Bose-Einstein distribution function. The phonon mean free path $\lambda(\omega)$ for backscattering is equivalent to $4/3v(\omega)\tau_{ph}(\omega)$ for three-dimensional (3D) $\boldsymbol{q}$-space [11], where $v(\omega)$ is the average phonon group velocity at a given frequency.

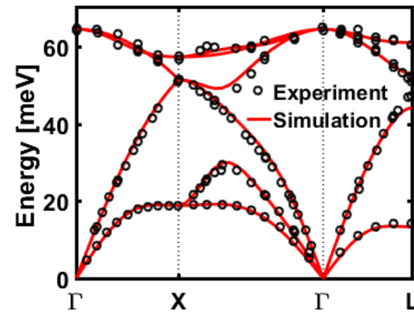

Fig. 1. Phonon band structure of Si calculated by the VFF model. The experimental data have been taken from Refs. [9] and [10].

The phonon relaxation time $\tau_{ph}(\omega)$ obeys Matthiessen's rule, its inverse being the sum of inverse lifetimes corresponding to each involved scattering process: anharmonic phonon-phonon ($B\omega^2 T e^{-C/T}$), impurity ($P\omega^4$), and crystalline boundary scattering ($v(\omega)/lF$). The crystalline boundary scattering mean free path ($l_b = lF$) is proportional to the shape and specularity of the sample boundary. The parameters B, C, and lF are derived by fitting the bulk thermal conductivity of Si to experimental data, while P is analytically determined from the difference in the isotope mass variations. Here, "bulk" refers to a large but finite sample used in the measurement of Ref. [12]. In nanowires, l_b is equal to the wire lateral dimension. All these parameters summarized in Table 1, nothing more, are used to predict the nanowire thermal conductivity.

C. Phonon surface roughness scattering

We follow the prescriptions of Ref. [6] based on scattering by a static strain field. The standard formula for time-dependent perturbation theory is employed. The transition probability from the initial state at momentum $\boldsymbol{q}$ and energy $E=\hbar\omega$ to final state of momentum $\boldsymbol{q}'$ and energy E' per unit time t due to the perturbed Hamiltonian H' is given by

$$\wp(\boldsymbol{q},\boldsymbol{q}') = \frac{2\pi}{\hbar}\left|\langle\boldsymbol{q}|H'|\boldsymbol{q}'\rangle\right|^2 \delta(E'-E). \quad (6)$$

This is known as Fermi's Golden Rule transition probability per unit time. In order to get the total rate of change, the summation over all modes $\boldsymbol{q}'$ is required. The volume $\boldsymbol{q}$-space summation can be reduced to the surface integral over dS' [7]. The total phonon scattering rate of a phonon branch i is the sum of the phonon scattering rate over all branches j

$$\frac{1}{\tau_i} = \sum_j \frac{1}{\tau_{i,j}} = \frac{2\pi}{\hbar}\sum_j \frac{V}{(2\pi)^3}\int_{\omega'=\omega_i} dS' \frac{\left|\langle\boldsymbol{q}|H'|\boldsymbol{q}'\rangle\right|^2}{v_{ph}^j(\omega')} \quad (7)$$

where V is the volume of the simulated device. The perturbation energy matrix element linking state $\boldsymbol{q}$ and $\boldsymbol{q}'$ due to the static strain field expressed in terms of 3D Fourier transformation of a space dilatation ($\Delta(\boldsymbol{r})$) is

$$\left|\langle\boldsymbol{q}|H'|\boldsymbol{q}'\rangle\right|^2 = \frac{4\gamma^2}{3V^2}\hbar^2\omega'^2\Lambda^2(\boldsymbol{q}'-\boldsymbol{q})$$
$$\Lambda(\boldsymbol{q}) = \int \Delta(\boldsymbol{r})e^{-i\boldsymbol{q}\cdot\boldsymbol{r}}d\boldsymbol{r} \quad (8)$$

Simulation of Semiconductor Processes and Devices 2016
Edited by E. Bär, J. Lorenz, and P. Pichler

TABLE I. SCATTERING MECHANISM PARAMETERS.

Scattering parameters	Constants	
	⟨100⟩ *orientation*	⟨111⟩ *orientation*
B	5.12×10^{-20} s/K	7.12×10^{-20} s/K
C	160 K	152 K
P	2.13×10^{-45} s^3	2.21×10^{-45} s^3
lF	1.07×10^{-2} m	6.62×10^{-3} m

where γ is the Grüneisen parameter.

We model roughness in Si nanowires assuming that their surface is distributed according to a Gaussian- or exponential-autocorrelation function $\Delta(\boldsymbol{r}_{//})$ with $\boldsymbol{r}_{//}$ as the position vector parallel to the surface.

$$\left\langle \Delta(\boldsymbol{r}_{//})\Delta(\boldsymbol{r}_{//} - \boldsymbol{r}'_{//})\right\rangle = \begin{cases} \Delta^2 e^{-r_{//}^2/L^2} & \text{Gaussian} \\ \Delta^2 e^{-\sqrt{2}\,r_{//}/L} & \text{Exponential} \end{cases} \tag{9}$$

The 3D Fourier transform of the space varying dilatations, $\Lambda(\boldsymbol{q})$, can be derived as follows for Gaussian- and exponential-functions

$$\Lambda^2(\boldsymbol{q}) = \begin{cases} \pi\Delta^4 L^2 e^{-q^2L^2/4} & \text{Gaussian} \\ \pi\Delta^4 L^2 / \left[1 + q^2L^2/2\right]^{3/2} & \text{Exponential} \end{cases}. \tag{10}$$

We will demonstrate here that both functions lead to a good reproduction of the nanowire thermal conductivity. We set L = 6 nm as previously proposed in Ref. [7] and as estimated from transmission electron microscope images [2]. The parameter Δ is varied to give the best possible fit to experimental data. Measurements suggest that the mean roughness height of the nanowire surface is typically comprised between 1-5 nm [2].

III. RESULTS

Our Si bulk and nanowire thermal conductivities show excellent agreement with experimental data, as illustrated in Fig. 2. In Fig. 2(b), we had to vary l_b, which is normally set to the nanowire diameter (d), from 1.00 d down to 0.35 d. In large nanowires, this variation can be justified because the actual cross-sectional area is not precisely known [5]. However, for d = 22 nm and below, a rigorous quantum-mechanical treatment is required, which is compensated here by a reduction in l_b.

As the surface per volume ratio increases, the effect of surface roughness becomes stronger. Figure 3 shows the reduction of the thermal conductivity due to surface roughness in comparison to an ideal nanowire. At room temperature, the thermal conductivity decreases by a factor of four when reducing the diameter from 115 nm to 50 nm and assuming a constant roughness amplitude of $\Delta \approx 1.8$ nm (Fig. 3(c)). This huge reduction can replace the l_b adjustment required by the 22 nm nanowire. Therefore, the accurate modeling of surface roughness is extremely important for sub-20nm widths in which quantum mechanics plays a significant role.

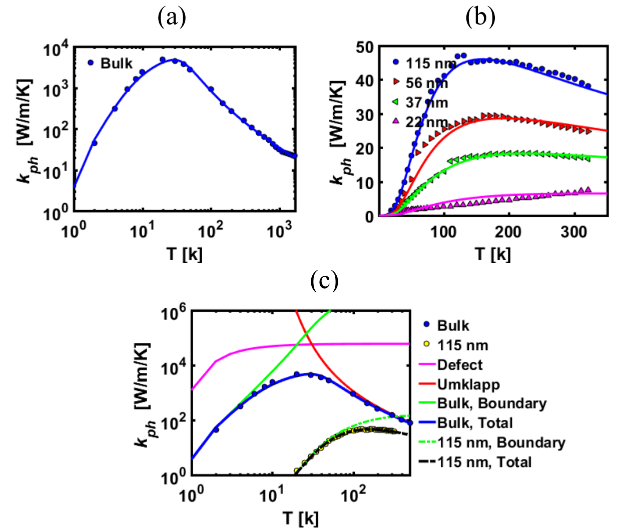

Fig. 2. Thermal conductivity of Si. (a) Bulk. (b) The ideal nanowires oriented in ⟨111⟩ direction, F = 1.00 for d = 115 and 56 nm, F = 0.80 for d = 37 nm, and F = 0.35 for d = 22 nm. (c) Contribution for each scattering process. Symbols refer to experimental data [2,12,13].

Exponential autocorrelation functions yield a slightly stronger reduction of the thermal conductivity than Gaussian ones, both for ⟨100⟩ and ⟨111⟩ directions (Figs. 3(a) and 3(b)). As a consequence, a larger Δ is required for the same reduction if L is kept constant. We also predict that engineering the surface roughness on Si nanowires grown in ⟨100⟩ direction should result in a stronger reduction of the thermal conductivity than in ⟨111⟩ direction at the same Δ, L, and d (see Figs. 3(a) and 3(b) at d = 115 nm).

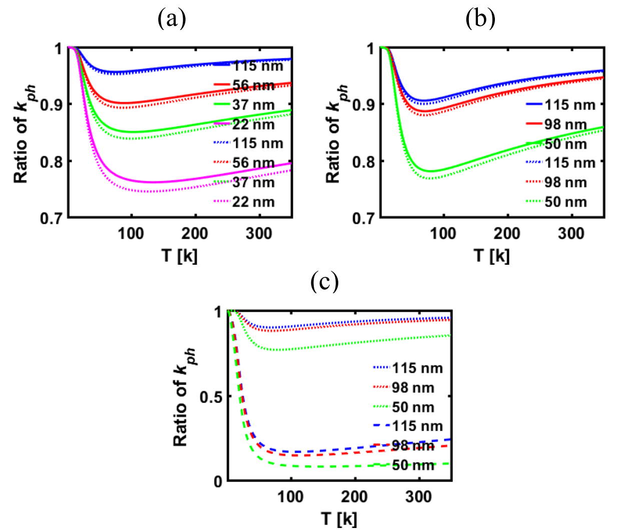

Fig. 3. Ratio of the thermal conductivities of nanowires with interface roughness and with perfectly smooth surface (Δ = 0 nm) computed by an exponential (dot and dash line) and Gaussian (solid line) correlation length, L = 6 nm. (a) Δ = 0.50 nm, nanowires in ⟨111⟩ direction. (b) Δ = 0.50 nm, nanowires in ⟨100⟩ direction. (c) Δ = 0.50 nm (dot line) and 1.75 nm (dash line), nanowires in ⟨100⟩ direction.

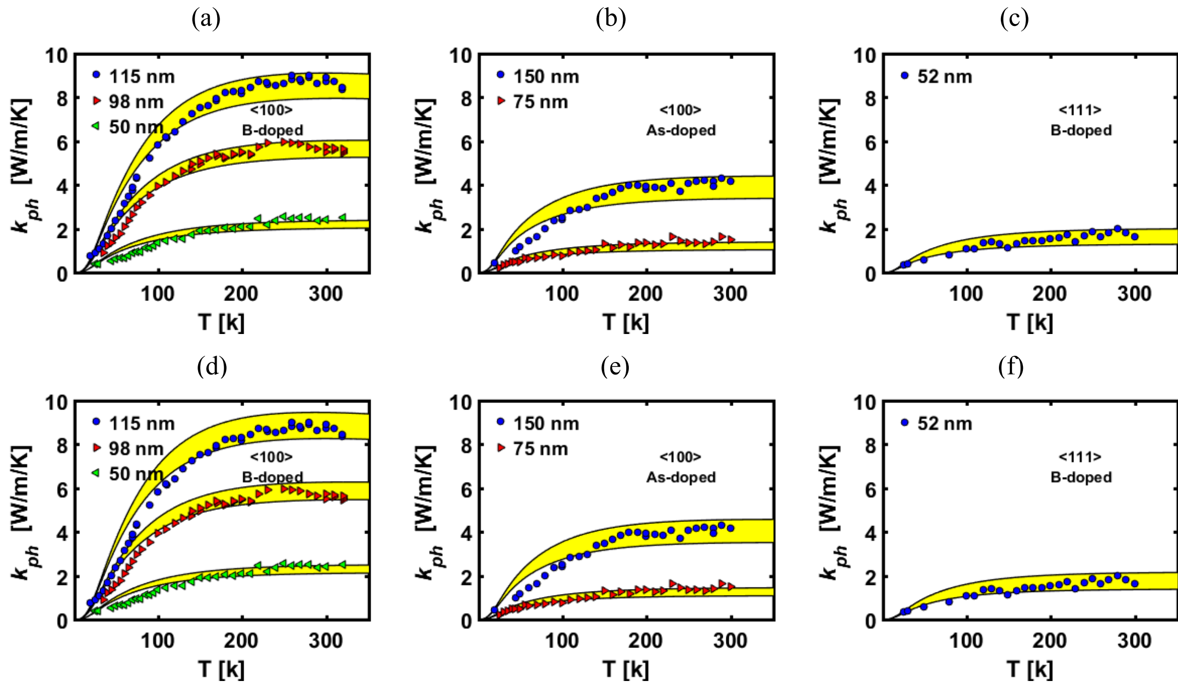

Fig. 4. Thermal conductivity of nanowires simulated with an exponential (a-c) and a Gaussian (d-f) distribution of their surface roughness characterized by a correlation length, L = 6 nm. (a, d) Δ = 1.52-1.75 nm. (b, e) Δ = 2.45-2.70 nm. (c, f) Δ = 2.15-2.50 nm. The symbols refer to experimental data [2]. Nanowires were synthesized from 10 Ωcm B-doped p-Si ⟨100⟩ (a, d), 0.01 Ωcm As-doped n-Si ⟨100⟩ (b, e), and 0.1 Ωcm B-doped p-Si ⟨111⟩ (c, f) wafers.

Simulations of the thermal conductivity of nanowires with rough surface and different crystal orientation are presented in Fig. 4. It is found that both exponential- and Gaussian-distributed roughness at the nanowire surface give almost the same thermal conductivity as expected. Although results for temperatures higher than 100 K have been significantly improved as compared to a previous study [7], our model cannot better predict the thermal conductivity at T < 100 K. This discrepancy comes from the fact that surface roughness scattering has little influence on the low-temperature thermal conductivity (Fig. 3). An increased Δ has a degressive influence on the thermal conductivity when the temperature decreases (Fig. 3(c)). In the low-temperature range, impurity and boundary scattering processes dominate (see Fig. 2(c)). They must therefore be carefully modeled, in particular in nanowires with a rough surface.

IV. Conclusion

We used the Landauer formula and the VFF model to compute the thermal conductivity of bulk Si and Si nanowires with and without interface roughness. In all cases, our model can well reproduce available experimental data. Due to its generality, it can be applied to predict the thermal conductivity in nanowires made of other materials such as InAs.

Acknowledgment

We acknowledge funding from the Swiss National Science Foundation through SNF under project 149454 (TORNAD).

References

[1] L. Zhao, et al., “Ultralow thermal conductivity and high thermoelectric figure of merit in SnSe crystals,” Nature, vol. 508, pp. 373-377, April 2014.

[2] A. I. Hochbaum, et al., “Enhanced thermoelectric performance of rough silicon nanowires,” Nature, vol. 451, pp. 163-167, January 2008.

[3] A. Boukai, et al., “Silicon nanowires as efficient thermoelectric materials,” Nature, vol. 451, pp. 168-171, January 2008.

[4] Z. Sui and I. P. Herman, “Effect of strain on phonons in Si, Ge, and Si/Ge heterostructures,” Phys. Rev. B, vol. 48, pp. 17938-17953, December 1993.

[5] N. Mingo, “Calculation of Si nanowire thermal conductivity using complete phonon dispersion relations,” Phys. Rev. B, vol. 68, pp. 113308, September 2003.

[6] P. G. Klemens, “Thermal conductivity and lattice vibrational modes,” Solid State Phys., vol. 7, pp. 1-98, 1958.

[7] P. Martin, Z. Aksamija, E. Pop, and U. Ravaioli, “Impact of phonon-surface roughness scattering on thermal conductivity of thin Si nanowires,” Phys. Rev. Lett., vol. 102, pp. 125503, March 2009.

[8] S. M. Goodnick et al., “Surface roughness at the Si(100)-SiO_2 interface,” Phys. Rev. B, vol. 32, pp. 8171-8186, December 1985.

[9] G. Nilsson and G. Nelin, “Study of the homology between silicon and germanium by thermal-neutron spectrometry,” Phys. Rev. B, vol. 6, pp. 3777-3786, November 1972.

[10] J. Kulda, D. Strauch, P. Pavone, and Y. Ishii, “Inelastic-neutron-scattering study of phonon eigenvectors and frequencies in Si,” Phys. Rev. B, vol. 50, pp. 13347-13354, November 1994.

[11] C. Jeong, S. Datta, and M. Lundstrom, “Thermal conductivity of bulk and thin-film silicon: a Landauer approach,” J. Appl. Phys., vol. 111, pp. 093708, May 2012.

[12] C. Glassbrenner and G. A. Slack, “Thermal conductivity of silicon and germanium from 3K to the melting point,” Phys. Rev., vol. 134, pp. A1058-A1069, May 1964.

[13] M. G. Holland, “Analysis of lattice thermal conductivity,” Phys. Rev., vol. 132, pp. 2461-2471, December 1963.